DOI: 10.1002/ejic.200500707

Mu-34: a New Porous Layered Fluorogallophosphate Material Obtained by in Situ Generation of Ethylamine

Louwanda Lakiss,[a] Angélique Simon-Masseron,[a] Florence Porcher,[b] and Joël Patarin*[a]

Keywords: Fluorogallophosphate / Ethylformamide / Solvothermal synthesis / Ethylamine / Porous layered solids / Microporous materials

A new two-dimensional microporous fluorogallophosphate with porous layers, named Mu-34, has been synthesized by in situ generation of ethylamine as the structure-directing agent, the latter arising from the decomposition of ethylformamide. The fluorogallophosphate Mu-34, $Ga_6P_8O_{32}FC_{14}N_7H_{56}$ (Z = 2), crystallizes in the triclinic space group $P\bar{1}$ with the following unit cell parameters: a = 11.0832(6), b = 11.393(6), c = 21.335(1) Å, α = 100.62(4), β = 99.66(5), γ = 108.34(5)°. The structure was solved from single crystal XRD data. This new fluorogallophosphate displays porous layers with apertures delimited by 12-membered rings intercalated by protonated ethylamine molecules. Mu-34 was also characterized by powder XRD, SEM, elemental and thermal analyses, and ^{13}C, ^{19}F, and ^{31}P MAS solid state NMR spectroscopy.

Introduction

Since the discovery of the microporous aluminophosphates by Wilson et al.,[1] research in the field of microporous materials has attracted considerable interest, owing to their potential uses as molecular sieves, heterogeneous catalysts, or ion exchangers.[2] The family of crystalline microporous phosphates is not limited to aluminophosphates; it also includes in particular zincophosphates and gallophosphates. These latter compounds allow a wide variety of structures to be formed, because gallium atoms can adopt 4-, 5-, and 6- coordinations. A main advance in the synthesis of these solids was achieved when fluoride anions were introduced in the starting mixture.[3] Thus, numerous fluorogallophosphates were obtained[4,5] such as cloverite, which was until now the molecular sieve with the largest 3D pore channel system.[6] In most cases F^- was found to be present in the inorganic framework as terminal Ga-F groups, bridging gallium atoms or trapped into small building units such as the so-called double four rings (D4R units). In the latter case it seems that fluorine, besides its mineralizing role, plays a templating role stabilizing these units.[5–8] To date, a large number of metallophosphates with 0D, 1D, 2D, or 3D frameworks have been reported.[3–13] Some of these solids were obtained through a newly developed synthesis route that consists of the in situ formation of the structure-directing agent (SDA).[9–13] In this synthesis route, alkylformamides are introduced as the main solvents in the starting mixture and during the synthesis they partly decompose into the corresponding amine which acts as a template and is occluded in the final material. With this method, it was possible to produce the two-layered aluminophosphates, Mu-4,[9] Mu-7[10] and, more recently, the three new gallophosphates MIL30,[11] Mu-30,[12] and Ea-TREN-GaPO.[13]

In this paper, we report the synthesis, structure determination, and characterization of a new porous 2D fluorogallophosphate named Mu-34 (Mu standing for Mulhouse), which was prepared in a quasi nonaqueous medium using ethylformamide (EFD) as the main solvent. As for the other solids described above, in this case too, the in situ formation of ethylamine seems to play a key role in the formation of this solid.

Results and Discussion

Synthesis and Crystal Morphology

The synthesis results are summarized in Table 1. The fluorogallophosphate Mu-34 crystallizes after 4 days at 200 °C (Table 1, sample A). With a similar starting molar composition but with a longer heating period (50 days) the gallophosphate ULM-3 was obtained as a pure phase (sample B). Such a result reveals the instability of Mu-34 in this reaction medium. Under these experimental conditions, it appears that the pH has to be high enough otherwise, whatever the gallium source (GaOOH or Ga_2O_3), the gallophos-

[a] Laboratoire de Matériaux à Porosité Contrôlée, UMR CNRS 7016, Université de Haute Alsace,
ENSCMu, 3 rue Alfred Werner, 68093 Mulhouse Cedex, France
[b] Laboratoire de Cristallographie et Modélisation des Matériaux Minéraux et Biologiques, UMR CNRS 7036, Faculté des Sciences, Université Henri Poincaré Nancy 1,
B. P. 239, 54506 Vandoeuvre-lès-Nancy Cedex, France

Supporting information for this article is available on the WWW under http://www.eurjic.org or from the author.

Table 1. Syntheses performed in the system GaOOH/H_3PO_4/HF/ethylformamide (EFD)/Tripropylamine (TPA)/H_2O.[a]

Sample (Heating time)	Molar composition of the starting mixture GaOOH	H_3PO_4	HF	EFD	H_2O[a]	TPA	T [°C]	XRD results
A (4 days)	2	2	1	10	4.7	1	200	Mu-34
B (50 days)	2	2	1	10	4.7	1	200	ULM-3
C (2 days)	2	2	1	10	4.7	–	200	Ea-TREN-GaPO + $GaPO_4$–C_4[b]
D (2 days)	2*	2	1	10	4.7	–	200	Ea-TREN-GaPO + $GaPO_4$–C_4[b]
E (50 days)	2	2	2	10	6.3	–	200	ULM-4 + impurity[c]

[a] H_2O arising from the orthophosphoric acid (85% H_3PO_4) and hydrofluoric acid (40% HF). [b] The two phases crystallize with the same proportion. [c] Unknown phase. * The gallium source was Ga_2O_3.

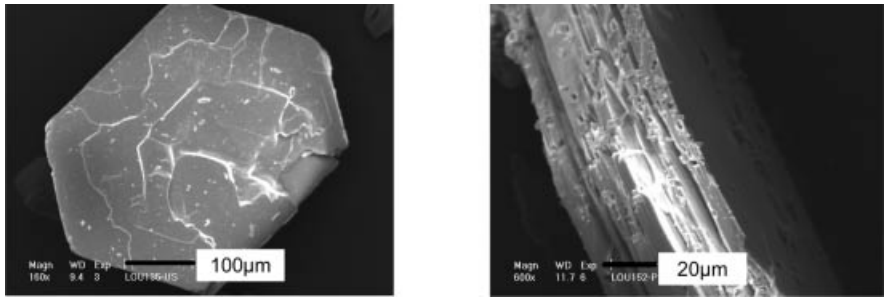

Figure 1. Scanning electron micrographs of the fluorogallophosphate Mu-34.

phates Ea-TREN-GaPO[13] and $GaPO_4$–C4[14] co-crystallize. This is clearly reflected by the experiments C and D performed in the absence of tripropylamine as a pH modifier. The presence of fluorine is also crucial. In its absence no crystalline phase is obtained. However, too large an amount leads to the formation of the gallophosphate ULM-4[15] (see sample E).

As can be seen in Figure 1, the crystals of Mu-34 display a pseudo-hexagonal shape. A close-up view shows that the crystals are in fact stacks of plate-like crystallites. This is indicative of a lamellar material.

XRD Analysis

The experimental powder diffraction pattern of the fluorogallophosphate Mu-34 is reported in part a of Figure 2 (a). From the single crystal XRD analysis, it has been indexed in a triclinic symmetry with the following unit cell parameters: a = 11.0832(6), b = 11.393(6), c = 21.335(1) Å, α = 100.62(4), β = 99.66(5), γ = 108.34(5)°. For comparison, the simulated XRD pattern of Mu-34 is reported in Figure 2 (b).

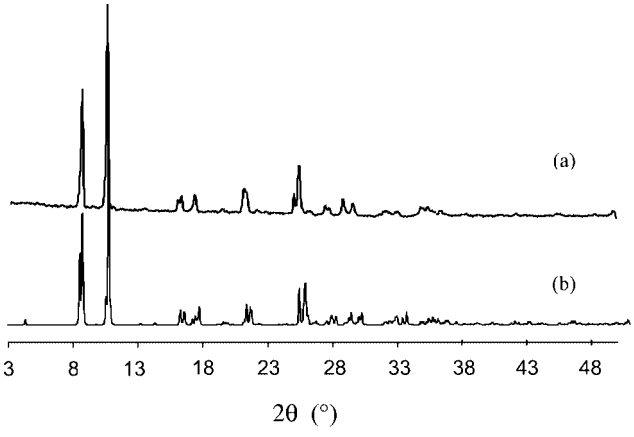

Figure 2. XRD patterns of the fluorogallophosphate Mu-34: (a) experimental pattern; (b) simulated pattern (radiation Cu-K_α1).

Chemical and Thermal Analyses

According to the elemental analyses, the as-synthesized Mu-34 sample has the following composition (wt.-%): Ga 27.46; P 15.56; F 1.57; N 6.19; C 10.74. Such results are in agreement with the composition obtained from the structure determination (wt.-%) Ga 27.20; P 16.11; F 1.26; N 6.37; C 10.93. The experimental C/N molar ratio equal to 2 is different from the value expected for ethylformamide (3C:1N), suggesting that the solvent partly decomposed into carbon monoxide and ethylamine (EA) during synthesis. This was later confirmed by ^{13}C NMR spectroscopy (see below). As previously shown for other phosphate-based materials synthesized in the presence of alkylformamide,[9–13] the in situ release of the corresponding protonated amine during the synthesis appears to be a key step in the crystallization of this lamellar gallophosphate. Indeed, experiments using ethylamine directly in the starting mixture led to the crystallization of the fluorogallophosphate ULM-3 with a nonidentified impurity.

The Ga/P molar ratio smaller than one (0.78 from chemical analyses, 0.75 from the structure determination) would indicate the presence of an interrupted framework, and more precisely the presence of terminal P=O and/or P–OH groups.

The thermal behavior of the fluorogallophosphate Mu-34 was investigated by TG/DTA thermal analyses. The TG and DTA curves of the as-synthesized fluorogallophosphate

Mu-34 are reported in Figure 3. The total weight loss occurs mainly in one step. However, a small weight loss close to 0.8 wt.-% appears before 200 °C. It might correspond to the loss of water molecules or fluorine (probably under the form of HF) since a weak and broad endothermic peak is observed on the DTA curve. The main weight loss (20.2 wt.-%), between 200 and 800 °C, is associated with at least three endothermic components on the DTA curve. This probably corresponds to desorption and decomposition of the organic template, to the removal of fluorine, and to the collapse of the gallophosphate framework. The exothermic signal, which is expected from the oxidation of the EA, is probably masked by the overwhelming endothermic collapse of the structure. The latter is confirmed by the XRD analysis of the residue left after heating to 800 °C, which shows that the starting material is transformed via an amorphization-recrystallization process into a cristobalite-type gallophosphate. This recrystallization might occur in two steps as reflected by the presence of two exothermic peaks on the DTA curve at 600 °C and 750 °C. Such a thermal behavior is often observed for microporous gallophosphates.[16] All of these analyses are in good agreement with the unit cell formula found by structure analysis: $[Ga_{12}(PO_4)_{16}F_2(C_2H_8N)_{14}]$.

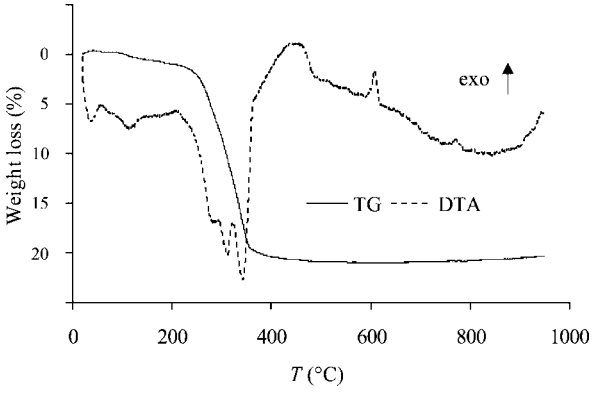

Figure 3. Thermal analysis (TG and DTA) under air of the fluorogallophosphate Mu-34.

Structure Description

The fluorogallophosphate Mu-34 displays a 2D structure composed of porous macroanionic layers, parallel to the {–111} faces of the crystal and containing 12-membered ring apertures (12MR) arranged in a pseudo-hexagonal way (Figure 4). The asymmetric unit (not reported) contains six crystallographically distinct Ga-sites, three in fourfold coordination with oxygen atoms (Ga1, Ga5, and Ga6) and three in fivefold coordination with four oxygen atoms and one fluorine (Ga2, Ga3, and Ga4). The GaO_4 tetrahedra exhibit a regular geometry, with an average Ga–O bond length of 1.81(±1) Å. The GaO_4F trigonal bipyramids have more disperse Ga–O bond lengths [<Ga–O> = 1.84(±3) Å] with three shorter bonds in the basal plane and a larger apical one, opposite to the Ga–F bond. Eight crystallographically distinct P-sites are also present: each phosphorus atom shares three of its oxygen atoms (labeled O1–O24) with gallium neighbors whereas the fourth oxygen atom (O25–O32) points towards the layer (Figure 5). The P–O distances involving these nonbonding oxygen atoms, 1.50(±1) Å, are typical of P=O bonds. They are significantly shorter than those involving bridging oxygen atoms [<P–O> = 1.54(±1) Å], except for O12 and O15 whose interaction with phosphorus is increased [P3–O12 = 1.503(6) Å, P4–O15 = 1.516(8) Å] as their bonding with gallium is weakened by

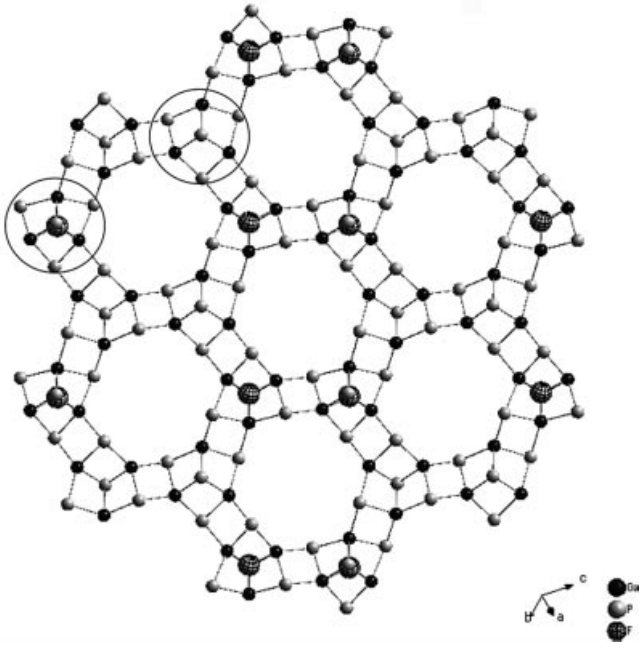

Figure 4. Projection of the structure of the fluorogallophosphate Mu-34 along the [–111] direction, showing the inorganic layers with the 12 MR openings. (For clarity, the oxygen atoms are omitted).

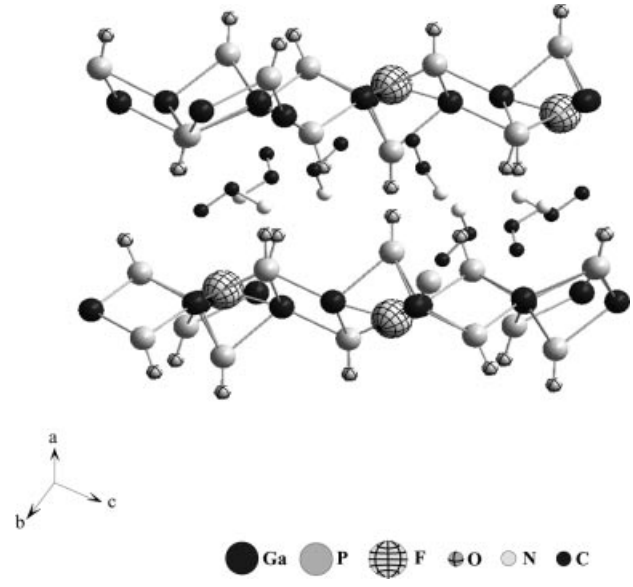

Figure 5. Projection of the structure of the fluorogallophosphate Mu-34, showing the localization of the protonated amine. (For clarity, the framework oxygen atoms are omitted except the terminal ones).

the presence of the supplementary fluoride ion. The crystal structure shows that all the terminal oxygen atoms act as hydrogen-bond acceptors for the seven crystallographically distinct protonated ethylamine molecules located in the interlayer space (Figure 5 and Figure 6). The positive charges of the organic molecules (see section ^{13}C NMR) compensate exactly the global negative charge of the layers if one considers formal P^{+5}, Ga^{+3}, O^{2-}, F^{-} ions. As expected, in protonated ethylamine molecules, the displacement parameters are smaller for the nitrogen atoms which are precisely in interaction with O=P groups. The water molecules, which might be observed by thermal analysis, were not detected by XRD, which is not surprising considering their predictable high mobility and low site occupancy factors.

The 12-membered ring porous anionic layers can be described as resulting from the connection of two types of building units, encircled in Figure 4, via four-membered rings ($Ga_2P_2O_4$). The first type of these building units (Figure 7, left) has already been observed in other 12 MR porous layered aluminophosphates.[17–19] It is a phosphate-capped six-membered ring ($Ga_3P_3O_6$) containing three tetracoordinate gallium atoms and four tetracoordinate phosphorus ones. The second building unit is original (Figure 7, right) and consists of a phosphate and fluorine (F1) capped six-membered ring. The six-membered ring is composed of three gallium and three phosphorus atoms located on crystallographic sites Ga2, Ga3, Ga4 and P6, P7, P8, respectively. These three gallium atoms are also connected to fluorine F1 and phosphorus P1 and adopt a distorted trigonal bipyramidal geometry, the angle between apical O–Ga–F angles ranging from 177.0(3) to 178.8(3)°. Fluorine is three-coordinate to gallium atoms with one short bond [*d*(Ga3–F) = 2.080(5) Å] and two long bonds [*d*(Ga4–F) = 2.274(5) Å and *d*(Ga2–F) = 2.402(6) Å]. Such bond lengths are larger than those previously found in other fluorogallophosphates[16] [typically $1.94 < d(\text{Ga–F}) < 2.04$ Å] but the presence of the third interaction could explain the difference between these values and those reported for ideal bonds.

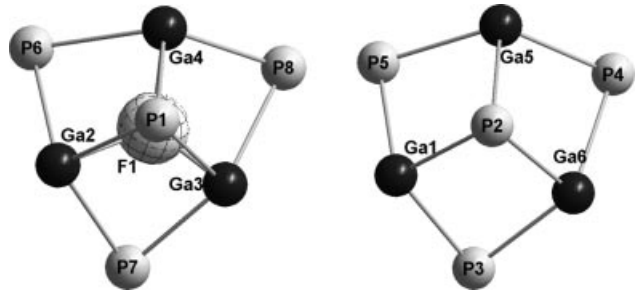

Figure 7. The two basic building units of the fluorogallophosphate Mu-34. (For clarity, the framework oxygen atoms are omitted).

^{13}C CP MAS NMR Spectroscopy

The ^{13}C CP MAS NMR spectrum of the fluorogallophosphate Mu-34 reported in Figure 8 shows two main

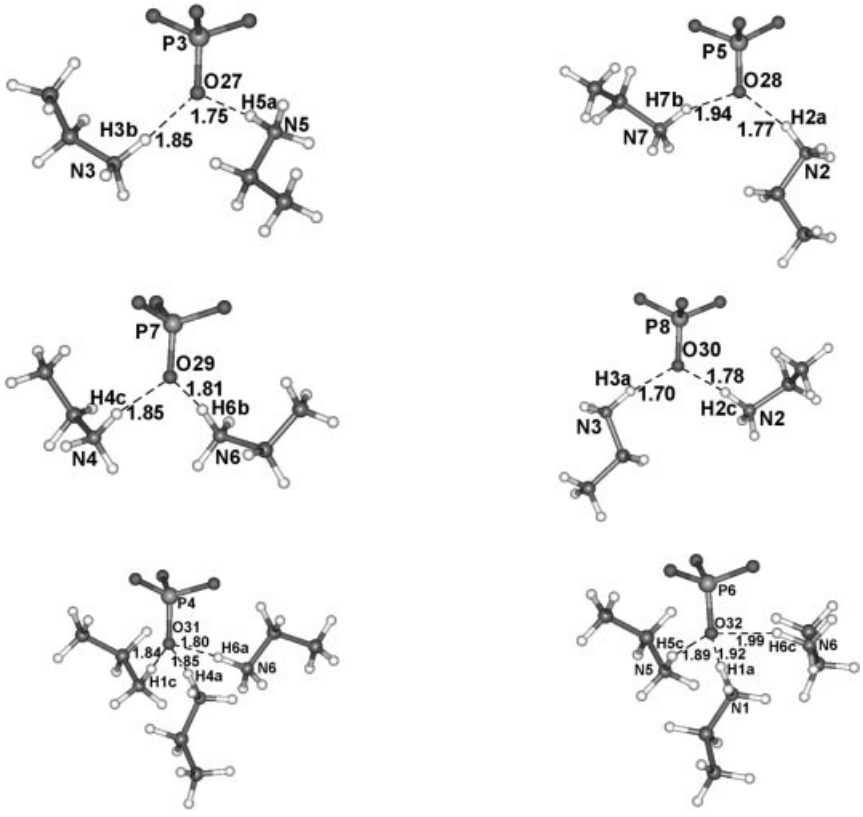

Figure 6. Hydrogen bonding scheme (dotted lines) for each phosphorus site.

peaks situated at δ = 15.0 and 36.4 ppm. They are assigned to the CH_3 and CH_2 groups of the ethylamine molecule, respectively.[20] No carbonyl group is observed on this spectrum (line expected at $\delta \approx 160$ ppm),[9] which means that EFD is decomposed into ethylamine (EA) and carbon monoxide under our experimental conditions. The ^{13}C isotropic chemical shifts for protonated and nonprotonated EA in the liquid state are at δ = 13 and 18 ppm, respectively for the methyl group, and at δ = 37 and 36 ppm, respectively for the CH_2 group. Thus, as suggested in the previous section, the EA occluded in Mu-34 appears to be protonated.

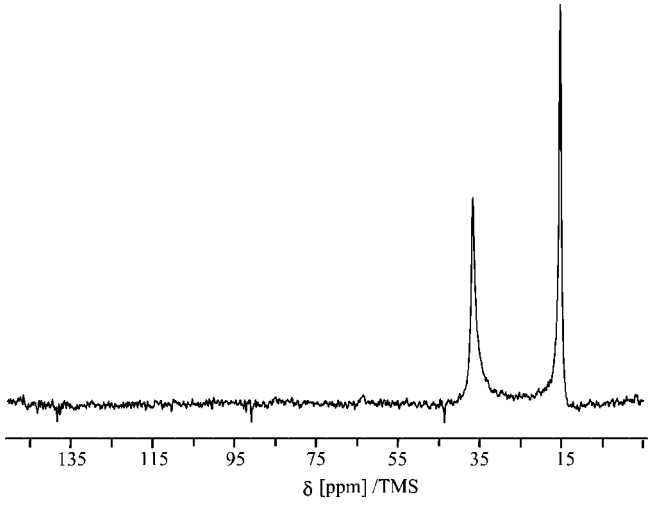

Figure 8. ^{13}C CP MAS NMR spectrum of the fluorogallophosphate Mu-34.

^{19}F MAS NMR Spectroscopy

The ^{19}F MAS NMR spectrum of the as-synthesized product, reported in Figure 9, exhibits one signal located at δ = –82 ppm. As observed for the gallophosphate Mu-28[16] and in good agreement with the crystal structure analysis, such a chemical shift value could be assigned to the three-coordinate fluorine atoms.

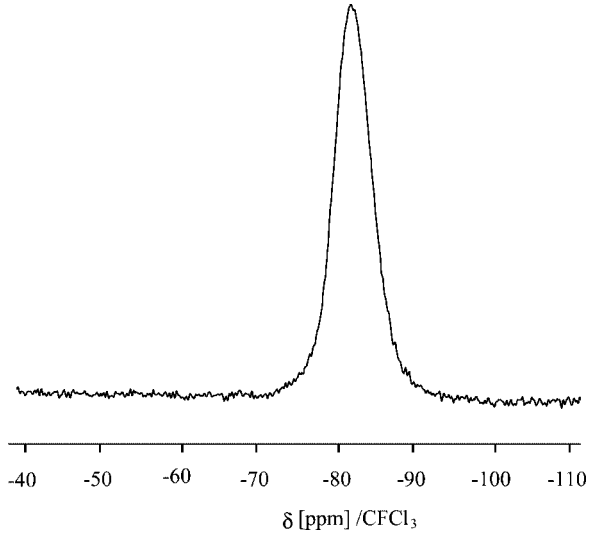

Figure 9. ^{19}F MAS NMR spectrum of the fluorogallophosphate Mu-34.

^{31}P MAS NMR Spectroscopy

The ^{31}P MAS NMR spectrum of the fluorogallophosphate Mu-34, shown in Figure 10, displays six signals at δ = 2, –2.3, –4.4, –6.6, –7.7, and –9.9 ppm. After decomposition, the relative areas are close to 1:1:1:2:1:2 respectively, indicating, in agreement with the structure determination, the existence of eight crystallographically distinct phosphorus sites. ^1H-^{31}P CP MAS NMR experiments have also been performed (spectrum not reported) and whatever the contact time (0.1, 0.05 ms) no significant difference was observed between the MAS and CP MAS spectra which means that all the atoms have the same proton environment. According to the structure and despite the low field chemical shift values observed no terminal P–OH group is present. Such a result is quite expected since all P atoms are hydrogen bonded via their P=O group (see Figure 6). A tentative assignment of the NMR peaks might be proposed on the basis of the empirical relationship between the ^{31}P isotropic chemical shift and the bond valence sum of the oxygen atoms connected to the phosphorus atom.[21] From the equation developed by Brown[22] and using the P–O and Ga–O bond lengths, the total oxygen bond valences [Σs(O)] including the contribution of the hydrogen bonds[23] for the phosphorus atoms P1, P2, P3, P4, P5, P6, P7, and P8 are equal to 8.04, 8.23, 8.27, 8.48, 8.35, 8.64, 8.29, and 8.27, respectively. Consequently, the assignment of the eight NMR peaks might be made as follows. The most highfield signal is attributed to the phosphorus atom, which has the highest oxygen bond valence. Therefore, the peak at δ = –9.9 ppm, which has a relative area close to 2, could be assigned to P6 and P4 respectively [Σs(O) = 8.48 for P4 and

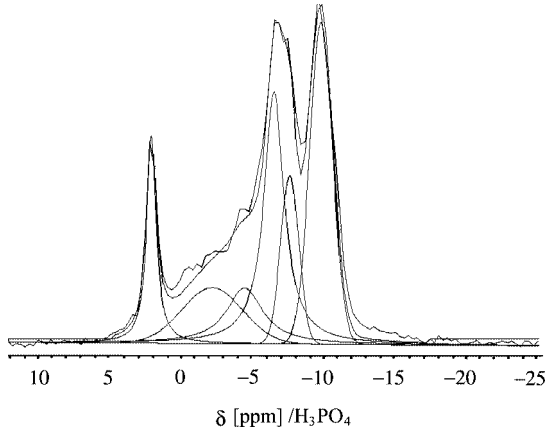

Figure 10. ^{31}P MAS NMR spectrum of the fluorogallophosphate Mu-34 and its decomposition.

8.64 for P6], the signal at δ = –7.7 ppm to P5 [Σs(O) = 8.35], and the signal at δ = 2 ppm to P1 [Σs(O) = 8.04]. Due to similar Σs(O) (8.23, 8.27, and 8.29), the other remaining signals are more difficult to assign.

Conclusions

In this paper the synthesis and characterization of a novel fluorogallophosphate Mu-34, with a rather unusual structure, has been reported. It was prepared in a quasi nonaqueous medium using ethylformamide as the main solvent. As in several similar syntheses, the solvent decomposed during the synthesis, and the corresponding amine was found to be occluded in the final structure. The in situ release of the protonated amine during the synthesis appears to be a key step in the crystallization of this lamellar gallophosphate. Indeed, experiments using ethylamine in the starting mixture directly did not lead to the crystallization of this material.

The fluorogallophosphate Mu-34 displays porous layers built up from 4-, 6-, and 12-membered rings and resulting from the connection of two types of building units: a phosphate-capped six-membered ring and a phosphate and fluorine capped six-membered ring. It is noteworthy that in this latter unit, the fluorine atom is three-coordinate to gallium atoms. In order to compensate the negative charges of the anionic layers protonated ethylamine molecules are intercalated between. These molecules interact strongly with the inorganic layers via hydrogen bonds.

Experimental Section

Synthesis: The fluorogallophosphate Mu-34 was prepared in a quasi nonaqueous fluoride medium at 200 °C from a mixture containing the ethylformamide as a precursor of the SDA (ethylamine). The molar composition of the starting mixture was 2 GaOOH : 2 H_3PO_4 : 1 HF : 10 ethylformamide (EFD) : 4.7H_2O. The amount of water arises from the phosphorus and fluoride sources. The pH value of the reaction mixture was adjusted to 4.5 with tripropylamine (TPA, Fluka 98 wt.-%), the latter presenting no structure-directing effect in the fluorine-containing gallophosphate system.[24] The amorphous gallium oxyhydroxide GaOOH was prepared by heating a gallium nitrate aqueous solution at 250 °C for 24 h. The other reactants were orthophosphoric acid (Labosi H_3PO_4 85 wt.-%), hydrofluoric acid (Prolabo HF 40 wt.-%), and EFD (Fluka 99 wt.-%). The starting mixture was prepared by adding the amorphous gallium source (1.13 g) to the ethylformamide (3.65 g) under magnetic stirring. Then orthophosphoric acid (1.15 g) and hydrofluoric acid (0.25 g) were introduced. In order to increase the pH value, tripropylamine was added (0.72 g) and the mixture was stirred until it was homogeneous. Then, it was transferred to a 20 mL PTFE-lined stainless-steel autoclave and heated at 200 °C for 4 days. The product was filtered, washed with distilled water and dried at 60 °C overnight.

Characterization: The as-synthesized product was characterized by powder X-ray diffraction (XRD) with a STOE STADI-P diffractometer equipped with a curved germanium (111) primary monochromator and a linear position-sensitive detector using Cu-K_α1 radiation (λ = 1.5406 Å). The morphology and average size of the crystals were determined by scanning electron microscopy (SEM) with a Philips XL30 microscope. Elemental analyses were carried out with the Induced Coupled Plasma technique using Atomic Energy Spectroscopy (ICP AES) for Ga and P, and by coulometric and catharometric methods for C and N quantifications, respectively. Thermogravimetric (TGA) and differential thermal (DTA) analyses were performed under air with a Setaram Labsys thermoanalyser with a heating rate of 5 °C min^{-1} up to 1000 °C. The ^{13}C CP MAS NMR spectrum was recorded with a Bruker MSL 300 spectrometer and the ^{19}F MAS, ^{31}P MAS, and ^{31}P CP MAS spectra with a Bruker DSX 400 spectrometer. The recording conditions are reported in Table 2. For the structure determination, a crystal plate was cut out of a larger aggregate and selected after optical examination under crossed polars. The single-crystal X-ray diffraction experiment was carried out at room temperature with an Oxford diffraction Xcalibur diffractometer equipped with a CCD detector. A full redundant Ewald sphere was collected with Mo-K_α radiation up to the maximum resolution $\sin\theta/\lambda_{max.}$ = 0.78 Å^{-1}. Bragg intensities were integrated with CrysAlis software,[25] and averaged in Laue group $P\bar{1}$ with the SORTAV program[26] after an absorption correction (μ = 3.633 mm^{-1}) based on the crystal shape. Data collection details are summarized in Table 3. The crystal structure was solved by direct methods using SHELXS[27] and refined with JANA2000.[28] The positions of all non-H atoms were found straightforwardly on successive Fourier maps. Hydrogen atoms were introduced in the structural model assuming ideal conformations for all protonated ethylamine molecules. Atomic displacement parameters of H atoms were restrained to 1.5 times the value of that of the heavy atom they were attached to. All bond lengths and bond angles of protonated ethylamine molecules were also restrained to the expected values observed in CH_3 (methyl), CH_2 (methylene), and NH_3 (amine) groups.[29] The refinement converged to R = 0.0575 ($R = \Sigma||F_o| - |kF_c||/\Sigma|F_o|$) and Rw = 0.0591 [$R_w = \{\Sigma w(|F_o| - |kF_c|)^2/\Sigma w(|F_o|^2)\}^{1/2}$] for 6644 reflections [$I > 3\sigma(I)$]. The supplementary crystallographic data are available online via http://www.fiz-karlsruhe.de (the reference file number is CSD-415650).

Table 2. Recording conditions of the NMR spectra.

	^{13}C CP MAS	^{31}P MAS	^{31}P CP MAS	^{19}F MAS
Chemical shift reference	TMS	85% H_3PO_4	85% H_3PO_4	$CFCl_3$
Frequency [MHz]	75.47	161.98	161.98	376.5
Pulse width [μs]	3.7	3.5	4.5	2
Flip angle	π /2	π /2	π /2	π /2
Contact time [ms]	1	/	0.05–0.1	/
Recycle time [s]	8	30	10	20
Spinning rate [Hz]	5000	25000	25000	25000
Number of scans	80	64	64	32

Table 3. Experimental single crystal XRD data and structure analysis of the fluorogallophosphate Mu-34.

	Mu-34
Chemical formula (asymmetric unit)	$[Ga_6(PO_4)_8F(C_2H_8N)_7]$
Cell parameters	a = 11.0832(6) Å, b = 11.393(6) Å, c = 21.335(1) Å α = 100.62(4)°, β = 99.66(5)°, γ = 108.34(5)°
V [Å^3]	2438.7(2)
Space group	$P\bar{1}$
Z	2
Crystal size [μm]	40 × 100 × 120
Diffractometer	Oxford diffraction Xcalibur 2 + Sapphire CCD
Radiation source, wavelength	Mo-K_α, λ = 0.71073 Å
Absorption coefficient [mm^{-1}]	3.633
Temperature [K]	293
Reflections measured, independent	90333, 17034
Observed reflections [$I > 3\sigma(I)$]	6644
Overall completeness ($\sin\theta/\lambda_{max.}$ = 0.78 Å^{-1})	88.7%
R_{int}	0.076
Structure refinement [$I > 3\sigma(I)$]	R = 0.0575, Rw = 0.0591, goof = 2.42

$$R_{int} = \frac{\sum_H \sqrt{N/N-1} \sum_i^{N_{equi}} |I_i - \langle I \rangle|}{\sum_H \sum_i^{N_{equi}} |I_i|}, \quad R = \left(\sum_H^o \left| |F_{obs}| - |kF_{calc}| \right| \right) \Big/ \left(\sum_H^o |F_{obs}| \right),$$

$$Rw = \left(\left(\sum_H^o w \left(|F_{obs}| - |kF_{calc}| \right)^2 \right) \Big/ \left(\sum_H^o w |F_{obs}|^2 \right) \right)^{1/2}, \quad Gof = \left(\left(\sum_H^o w \left(|F_{obs}| - |kF_{calc}| \right)^2 \right) \Big/ (m-n) \right)^{1/2},$$

$w = 1/\sigma^2(F_{obsd.})$, m is the number of reflections used, n the number of parameters

Supporting Information (see footnote on the first page of this article): Tables S1–S3 of atomic coordinates, displacement parameters, selected bond lengths and angles.

[1] S. T. Wilson, B. M. Lok, C. A. Messina, T. R. Cannan, E. M. Flanigen, *J. Am. Chem. Soc.* **1982**, *104*, 1146.
[2] M. E. Davis, *Nature* **2002**, *417*, 813.
[3] H. Kessler, J. Patarin, C. Schott-Darie, in *Advanced Zeolite Science and Applications, Studies in Surface Science and Catalysis* (Eds.: J. C. Jansen, M. Stöcker, H. G. Karge, J. Weitkamp), Elsevier, Amsterdam, **1994**, vol. 85, p.75.
[4] G. Férey, *J. Fluorine Chem.* **1995**, *72*, 187.
[5] J. Patarin, J. L. Paillaud, H. Kessler, in *Synthesis of AlPO$_4$s and other crystalline materials, Handbook of Porous Solids* (Eds.: F. Schüth, K. S. W. Sing, J. Weitkamp), Wiley-VCH, Germany, **2002**, ch. 4.2.3, vol. 2, p. 815.
[6] M. Estermann, L. B. McCusker, Ch. Baerlocher, A. Merrouche, H. Kessler, *Nature* **1991**, *352*, 320.
[7] A. Matijasic, P. Reinert, L. Josien, A. Simon, J. Patarin, in *Zeolites and Mesoporous Materials at the Dawn of the 21st Century, Studies in Surface Science and Catalysis* (Eds.: A. Galarneau, F. Direnzo, F. Fajula, J. Vedrine), Elsevier, Amsterdam, **2001**, vol. 135, p. 142.
[8] P. Caullet, J. L. Paillaud, A. Simon-Masseron, M. Soulard, J. Patarin, *C. R. Chimie* **2005**, *8*, 245.
[9] L. Vidal, V. Gramlich, J. Patarin, Z. Gabelica, *Eur. J. Solid State Inorg. Chem.* **1998**, *35*, 545.
[10] L. Vidal, V. Gramlich, J. Patarin, Z. Gabelica, *Chem. Lett.* **1999**, 201.
[11] C. Paulet, T. Loiseau, G. Férey, *J. Mat. Chem.* **2000**, *10*, 1225.
[12] L. Lakiss, A. Simon-Masseron, V. Gramlich, J. Patarin, *Solid State Sci.* **2005**, *7*, 141.
[13] L. Lakiss, A. Simon-Masseron, J. Patarin, *Micro. Meso. Mater.* **2005**, *84*, 50.
[14] S. Feng, R. Xu, *Chem. J. Chinese Univ.* **1988**, *4*, 1.
[15] T. Loiseau, F. Taulelle, G. Férey, *Micro. Mater.* **1997**, *9*, 83.
[16] L. Josien, A. Simon-Masseron, V. Gramlich, F. Porcher, J. Patarin, *J. Solid State Chem.* **2004**, *177*, 3721.
[17] J. M. Thomas, R. H. Jones, R. Xu, J. Chen, A. M. Chippindale, S. Natarajan, A. K. Cheetham, *J. Chem. Commun.* **1992**, 929.
[18] A. M. Chippindale, A. R. Cowley, Q. Huo, R. H. Jones, A. D. Law, J. M. Thomas, R. Xu, *J. Chem. Soc. Dalton Trans.* **1997**, 2639.
[19] P. A. Barrett, R. H. Jones, *J. Chem. Commun.* **1995**, 1979.
[20] H. O. Kalinowski, S. Berger, S. Braun, *^{13}C NMR Spektroskopie*, Thieme, Stuttgart, **1984**, 189.
[21] A. K. Cheetham, N. J. Clayden, C. M. Dobson, J. B. Jakeman, *J. Chem. Soc. Chem. Commun.* **1986**, 195.
[22] I. D. Brown, *Structure and Bonding in Crystals*, Academic Press, New York, **1981**, ch. 14, vol. 2, p. 1.
[23] I. D. Brown, D. Altermatt, *Acta Crystallogr. Sect. B* **1985**, *41*, 244.
[24] C. Schott-Darie, Ph. D. Thesis, University of Haute Alsace, Mulhouse, **1994**.
[25] *CrysAlis* Software System, Version 1.170, Oxford Diffraction Ltd, **2003**.
[26] R. H. Blessing, *J. Appl. Cryst.* **1997**, *30*, 421.
[27] G. M. Sheldrick, *SHELXS86*, Program for the Solution of Crystal Structures, University of Göttingen, Germany, **1986**.
[28] V. Petříček, M. Dušek, *The Crystallographic Computing System JANA2000*, Institute of Physics, Praha, Czech Republic, **2000**.
[29] *International Tables for X-ray Crystallography*, Kluwer Academic Publishers, Dordrecht, vol. C, **1992**.

Received: August 5, 2005
Published Online: November 17, 2005

